ChemComm

COMMUNICATION

View Article Online
View Journal | View Issue

# Control of cytochrome *c* redox reactivity through off-pathway modifications in the protein hydrogen-bonding network†

Cite this: *Chem. Commun.*, 2014, **50**, 5355

Received 15th October 2013,
Accepted 16th December 2013

DOI: 10.1039/c3cc47943a

www.rsc.org/chemcomm

Jie Gu,[a] Soyeun Yang,[a] Alexander J. Rajic,[b] Igor V. Kurnikov,[c] Tatiana R. Prytkova[b] and Ekaterina V. Pletneva*[a]



**Measurements of photoinduced $Fe^{2+}$-to-$Ru^{3+}$ electron transfer (ET), supported by theoretical analysis, demonstrate that mutations off the dominant ET pathways can strongly influence the redox reactivity of cytochrome *c*. The effects arise from the change in the protein dynamics mediated by the intraprotein hydrogen-bonding network.**

Cytochrome *c* (cyt *c*), a small α-helical heme protein involved in oxidative phosphorylation, has become a workhorse for understanding the protein electron transfer (ET).[1] Its studies, as well as work on other systems, have suggested that the protein structure facilities ET,[2–5] but the nature of this effect has been controversial.[6] Herein, we present experimental results and theoretical analyses of a series of mutants of iso-1 yeast cyt *c* that not only point to the involvement of a specific ET pathway but also suggest the role of a distant site in alteration of electronic couplings through changes in the hydrogen-bonding network. Relevant to function, such changes could modulate the protein redox reactivity in response to its interactions with other proteins or biological membranes.

The highly conserved Y67 plays a key role in the structure and function of cyt *c*. Mutations at this site change the heme redox potential and protein stability.[7–11] This residue has also been suggested to trigger conformational rearrangements that enhance the peroxidase activity of cyt *c*, a transformation critical in early stages of apoptosis.[12] The interaction between the hydroxyl of Y67 and the sulfur of M80 is a part of the hydrogen-bonding network that connects folding units of low thermodynamic stability (Fig. 1).[9,11,13] Mutations Y67F, as well as N52I and N52I/Y67F, disrupt this network; the stability data and structural characterization of these variants are available.[7–9,11]

We have prepared four variants of cyt *c* with the above mutations, all having also a Cys residue at position 66. This Cys residue was labeled with the $Ru(bpy)_2(phen\text{-}IA)^{2+}$ complex. The combined effects of the Cys mutation and labeling do not significantly perturb the protein heme environment, secondary structure, or thermal stability (Fig. S1 and S2, and Table S1, ESI†). An absorption band at around 695 nm in all the ferric variants is consistent with Met being an axial ligand to the heme. The slight red shift and increase in intensity of this band for Y67F and

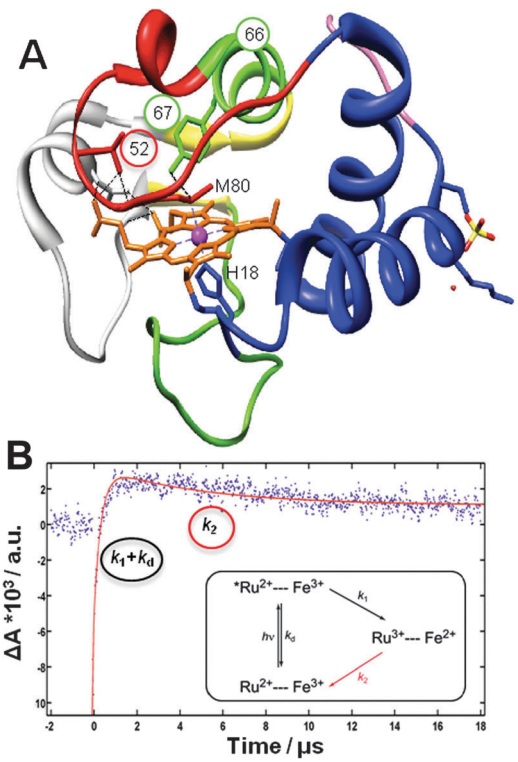


Fig. 1 (A) Structure of iso-1-cyt *c* (PDB file: 1YCC).[18] Heme group, heme ligands, and mutated residues are highlighted. Dashed lines illustrate the intraprotein hydrogen-bonding network, in which residues 52 and 67 participate. Units of different thermodynamic stability (foldons,[13] in order of increasing stability) are color-coded gray (nested-yellow, residues 40–57), red (residues 71–85), yellow (residues 37–39 and 58–61), green (60's helix and 20's–30's Ω loop), and blue (N- and C-terminal helices). (B) Transient absorption at 550 nm of $Ru^{66}$-E66C/Y67F (15 μM) after laser flash excitation and fit (smooth red line).

[a] *Department of Chemistry, Dartmouth College, Hanover, NH 03755, USA. E-mail: ekaterina.pletneva@dartmouth.edu; Tel: +1-603-646-0933*
[b] *Schmid College of Science & Technology, Chapman University, Orange, CA 92866, USA*
[c] *Department of Chemistry, Carnegie Mellon University, Pittsburgh, PA 15213, USA*

† Electronic supplementary information (ESI) available: Materials and methods; eleven figures and two tables. See DOI: 10.1039/c3cc47943a

Table 1 ET parameters for $Ru^{66}$-labeled variants of yeast iso-1 ferrocyt *c*

| Variant[a] | $k_2$[b] ($\mu s^{-1}$) | $\langle H_{DA}^2 \rangle^{1/2}$[c] (eV) | Calc. $k_{max}$ ($\mu s^{-1}$) | d (edge-to-edge)[d] (Å) | d (Ru-to-Fe)[d] (Å) |
|---|---|---|---|---|---|
| $Ru^{66}$-E66C | 0.12 ± 0.01 | $1.40 \times 10^{-6}$ | 0.033 | 12.3 | 22.3 |
| $Ru^{66}$-N52I/E66C | 0.10 ± 0.01 | $1.22 \times 10^{-6}$ | 0.025 | 13.2 | 22.8 |
| $Ru^{66}$-E66C/Y67F | 0.38 ± 0.08 | $1.93 \times 10^{-6}$ | 0.063 | 12.8 | 22.5 |
| $Ru^{66}$-N52I/E66C/Y67F | 0.12 ± 0.01 | $1.32 \times 10^{-6}$ | 0.029 | 12.3 | 21.5 |

[a] Also contains two background mutations K72A and C102S associated with WT*. [b] Rate constants for $Fe^{2+}$-to-$Ru^{3+}$ ET, measured in a sodium phosphate buffer at pH 7.4 by direct photoexcitation of the covalently-attached Ru complex. [c] Root-mean-square value. [d] From constructed models.

N52I/Y67F variants are in accord with previous reports and have been ascribed to the absence of the hydrogen bond between F67 and M80.[14] Trends in thermodynamic stability obtained from thermal denaturation experiments mirror those of the unlabeled variants (Table S1, ESI†):[8] the mutations increase the stability of the protein in both oxidation states, except for $Ru^{66}$-E66C/Y67F, whose stability is the same as that of $Ru^{66}$-E66C.

The rate constants $k_2$ for $Fe^{2+}$-to-$Ru^{3+}$ ET (Table 1) have been determined by transient absorption measurements after photoexcitation of the covalently-attached Ru complex (Fig. 1B and Fig. S3–S6). These experiments have monitored the kinetics at wavelengths characteristic of the heme (424 and 550 nm) and the Ru complex (450 nm). The values of $k_2$ for all the variants are the same within the error bounds, except for $Ru^{66}$-E66C/Y67F, whose rate constant $k_2$ is three-fold larger. Previous studies have found a similar acceleration of the photoinduced[15] and heterogeneous[10] ET rates upon the Y67F mutation in cyt *c*. Recent electrochemical work has attributed this rate increase in part to a decrease in the ET reorganizational energy $\lambda$ by ~0.1 eV in the mutant.[10] However, with a large $\lambda$ of ~1 eV, which is dominated by the solvent rearrangement around the Ru complex in our photoinduced reactions, this effect is a minor contributor. Furthermore, the change in $\lambda$ alone does not explain the peculiar lack of rate increase for $Ru^{66}$-N52I/E66C/Y67F, which also has the Y67F mutation.

To rationalize the effects of these mutations on the ET reactivity of cyt *c*, we have employed molecular dynamics (MD) and quantum mechanical calculations[16,17] to compute the Ru–Fe electronic coupling in the four variants. The protein conformational flexibility was taken into account with analyses of various snapshots along MD trajectories. Starting models of labeled cyt *c* derivatives were constructed on the basis of the crystal structure of the ferrous wild-type protein.[18] Solvation was treated explicitly with TIP3P water molecules and MD simulations were performed. Crystallographic studies have revealed the presence of an internally bound water molecule next to residues 52 and 67, which disappears with the N52I mutation.[9] Similar to crystallographic results, we observed a water molecule in this location in $Ru^{66}$-E66C and $Ru^{66}$-E66C/Y67F. This water moves outside of the protein during MD simulations of $Ru^{66}$-N52I/E66C and $Ru^{66}$-N52I/E66C/Y67F (Fig. S7, ESI†).

With similar edge-to-edge distances in all the variants (Table 1), the distinct ET rate for $Ru^{66}$-E66C/Y67F argues against a simple exponential model.[19] Instead, the results suggest the involvement of a specific pathway(s) influenced by the mutation of residue 67. A pathway-searching algorithm[20] has yielded identical dominant ET pathways (Fig. 2A) for all four variants consisting of σ bonds and a through-space jump (either from Cδ or Cε of residue 67). *Ab initio* quantum methods[16,17] were then used to calculate the mean square electronic couplings $\langle H_{DA}^2 \rangle$ in the protein fragments representing these pathways

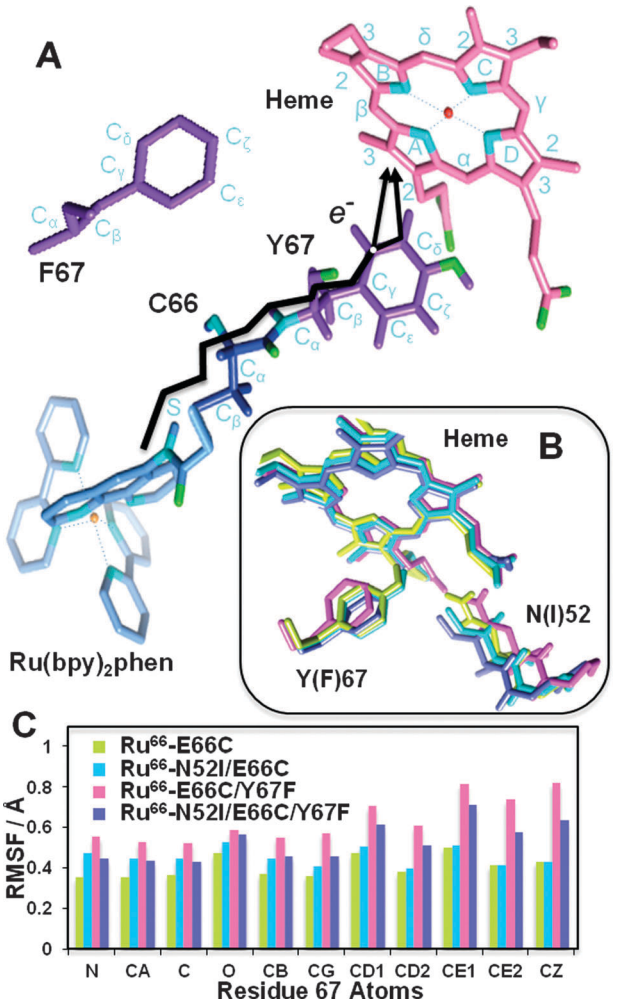


Fig. 2 (A) The protein fragment along the two dominant ET pathways. (B) Positions of the heme, residues 52 and 67, and (C) root mean square fluctuations (RMSF) of atoms in Y(F)67 for $Ru^{66}$-E66C (green), $Ru^{66}$-N52I/E66C (cyan), $Ru^{66}$-E66C/Y67F (pink), and $Ru^{66}$-N52I/E66C/Y67F (blue) from MD simulations.

from the many sampled MD snapshots. These detailed computations have also included the analysis of solvation. Assuming $-\Delta G^\circ = \lambda = 1.0$ eV, we have calculated nonadiabatic ET rates $k_{max}$ (Table 1).[2] The computed and observed rates agree within a factor of six; this order of magnitude agreement reflects a satisfactory description of the experiment with theoretical methods.[6] Importantly, the calculations reproduce remarkably well the increase in the ET rate for the $Ru^{66}$-E66C/Y67F variant. These consistencies suggest that differences in electronic couplings are responsible for the rate enhancement in this variant and point to the critical role of residue 67 in ET of $Ru^{66}$-labeled cyt *c* variants.

 

Analyses of crystal structures[7,9,18] have revealed only minor variations in the position of the aromatic residue 67 upon mutations (Table S2, ESI†). Temperature factors for atoms involved in the pathway slightly increase, particularly for the two variants having N52I mutation (Fig. S8, ESI†). However, the effects observed in the crystal may deviate from those in solution. Interestingly, MD simulations reveal increased mobility of the side chain of residue 67 for $Ru^{66}$-E66C/Y67F and $Ru^{66}$-N52I/E66C/Y67F compared to the two other variants (Fig. 2C). These changes are in accord with a recent study of horse heart Y67F cyt *c*[10] and likely result from the disruption of the Y67–M80 interaction as well as perturbations in the position of other amino acids and water molecules (Fig. S7, ESI†). The fluctuations in the protein structure translate into fluctuations in electronic couplings (Fig. S9, ESI†). Even though the average distance for the nonbonded jump for the dominant pathway does not change much upon Y67F mutation (Table S2, ESI†), the alterations in the protein structure enable sampling of Ru–Fe configurations with different superexchange interactions through the aromatic ring of residue 67 (Fig. S10, ESI†). For $Ru^{66}$-E66C/Y67F, the average orientation of the aromatic ring is notably different (see torsional angles in Table S2, ESI†). Collectively, the changes in structure and dynamics in this variant allow for a more favorable overlap between molecular orbitals of the heme and the aromatic ring of residue 67, leading to better overall electronic coupling and a faster ET rate (Fig. S10, ESI†).

The additional N52I mutation in $Ru^{66}$-N52I/E66C/Y67F reverses the effects of the Y67F replacement, as the aromatic ring readjusts and fluctuations of this side chain somewhat diminish (Fig. 2C). Offering a rationale to experimental ET rates, calculations reveal a decrease in the mean square electronic coupling for this variant. Resonance Raman studies of similar iso-1 ferrocyt *c* mutants N52V, Y67F, and N52V/Y67F have suggested deformation of the porphyrin ring in Y67F and N52V/Y67F mutants.[21] Alterations in the heme geometry as well as variations in the position of heme atoms among sampled snapshots are apparent in the model structures of Ru-labeled mutants (Fig. S11, ESI†). Quantum chemical calculations on Ru(bpy)-heme fragments from many snapshots explicitly account for both of these changes in calculations of electronic couplings.

Our experimental results, supported by electronic coupling calculations, convincingly demonstrate that the N52I mutation, off the dominant ET pathway, can have a strong influence on the ET reactivity of cyt *c*. Interestingly, on its own, the N52I replacement in $Ru^{66}$-N52I/E66C does not affect the Ru–Fe electronic coupling and the ET rate, compared to those in $Ru^{66}$-E66C. However, when coupled to the Y67F mutation, it exerts a sizeable effect on the ET rate, eliminating the rate enhancement of the Y67F replacement alone. The link here appears to be a change in the protein dynamics and possibly also deformation of the heme.

In their analysis of protein stability, Redzic and Bowler have shown negative cooperativity between N52I and Y67F mutations in ferric cyt *c*.[11] Combined, the two mutations weaken the interactions that optimally stabilize each of the two single mutants, suggesting communication between these two sites. The tightening of the protein internal cavity and associated displacement of internal water upon the N52I mutation (Fig. S7, ESI†) likely contributes to the adjustments of residue 67 (Fig. 2B and Table S2, ESI†) observed here, ultimately leading to effects on ET rates.

Propagation of structural changes through intraprotein hydrogen-bonding networks is an intriguing property of many signaling proteins.[22,23] The results herein suggest that such networks could also mediate changes in protein redox reactivity. The role of protein–protein interactions in modulating ET properties of cyt *c* has been a subject of very recent investigations that argue for a dynamic link between the heme and the protein surface.[24] Although residue 52 does not directly interact with cyt *c* redox partners,[25–27] it has been implicated in physiological binding to cardiolipin-containing membranes.[28] Furthermore, the extensive hydrogen-bonding network in cyt *c* links several other surface residues closer to the binding sites for cyt *c* redox partners,[25–27] whose effects on protein dynamics and ET reactivity would be interesting to explore.

This work was supported by the NSF CAREER grant CHE-0953693 (E.V.P) and Dartmouth Women-in-Science Project (S.Y.). We thank Bruce E. Bowler and Alexandre A. Pletnev for the Rbs(WT*) plasmid and synthesis of the Ru labeling reagent, respectively.

## Notes and references

1 *Cytochrome c* - A Multidisciplinary Approach, ed. R. A. Scott and A. G. Mauk, University Science Books, Sausalito, CA, 1996.
2 R. A. Marcus and N. Sutin, *Biochim. Biophys. Acta*, 1985, **811**, 265–322.
3 H. B. Gray and J. R. Winkler, *Biochim. Biophys. Acta*, 2010, **1797**, 1563–1572.
4 J. Wei, H. Liu, D. E. Khoshtariya, H. Yamamoto, A. Dick and D. H. Waldeck, *Angew. Chem., Int. Ed.*, 2002, **41**, 4700–4703.
5 M. D. Liptak, R. D. Fagerlund, E. C. Ledgerwood, S. M. Wilbanks and K. L. Bren, *J. Am. Chem. Soc.*, 2011, **133**, 1153–1155.
6 T. R. Prytkova, I. V. Kurnikov and D. N. Beratan, *Science*, 2007, **315**, 622–625.
7 A. M. Berghuis, J. G. Guillemette, M. Smith and G. D. Brayer, *J. Biol. Chem.*, 1994, **235**, 1326–1341.
8 C. M. Lett, A. M. Berghuis, H. E. Frey, J. R. Lepock and J. G. Guillemette, *J. Biol. Chem.*, 1996, **271**, 29088–29093.
9 A. M. Berghuis, J. G. Guillemette, G. McLendon, F. Sherman, M. Smith and G. D. Brayer, *J. Mol. Biol.*, 1994, **236**, 786–799.
10 D. Alvarez-Paggi, M. A. Castro, V. Tórtora, L. Castro, R. Radi and D. H. Murgida, *J. Am. Chem. Soc.*, 2013, **135**, 4389–4397.
11 J. S. Redzic and B. E. Bowler, *Biochemistry*, 2005, **44**, 2900–2908.
12 T. Ying, Z. H. Wang, Y. W. Lin, J. Xie, X. Tan and Z. X. Huang, *Chem. Commun.*, 2009, 4512–4514.
13 M. M. G. Krishna, Y. Lin, J. N. Rumbley and S. W. Englander, *J. Mol. Biol.*, 2003, **331**, 29–36.
14 M. M. Frauenhoff and R. A. Scott, *Proteins: Struct., Funct., Genet.*, 1992, **14**, 202–212.
15 D. R. Casimiro, J. H. Richards, J. R. Winkler and H. B. Gray, *J. Phys. Chem.*, 1993, **97**, 13073–13077.
16 I. V. Kurnikov and D. N. Beratan, *J. Chem. Phys.*, 1996, **105**, 9561.
17 M. R. Hartings, I. V. Kurnikov, A. R. Dunn, J. R. Winkler, H. B. Gray and M. A. Ratner, *Coord. Chem. Rev.*, 2010, **254**, 248–253.
18 A. M. Berghuis and G. D. Brayer, *J. Mol. Biol.*, 1992, **223**, 959–976.
19 J. J. Hopfield, *Proc. Natl. Acad. Sci. U. S. A.*, 1974, **71**, 3640–3644.
20 T. R. Prytkova, I. V. Kurnikov and D. N. Beratan, *J. Phys. Chem. B*, 2005, **109**, 1618–1625.
21 R. Schweitzer-Stenner, Q. Huang, A. Hagarman, M. Laberge and C. J. Wallace, *J. Phys. Chem. B*, 2007, **6527–33**, 6527–6533.
22 E. V. Pletneva, M. Sundd, D. B. Fulton and A. H. Andreotti, *J. Mol. Biol.*, 2006, **357**, 550–561.
23 P. A. Sigala, M. A. Tsuchida and D. Herschlag, *Proc. Natl. Acad. Sci. U. S. A.*, 2009, **106**, 9232–9237.
24 M. G. Galinato, J. G. Kleingardner, S. E. Bowman, E. E. Alp, J. Zhao, K. L. Bren and N. Lehnert, *Proc. Natl. Acad. Sci. U. S. A.*, 2012, **109**, 8896–8900.
25 C. Lange and C. Hunte, *Proc. Natl. Acad. Sci. U. S. A.*, 2002, **99**, 2800–2805.
26 H. Pelletier and J. Kraut, *Science*, 1992, **258**, 1748–1755.
27 V. A. Roberts and M. E. Pique, *J. Biol. Chem.*, 1999, **274**, 38051–38060.
28 M. Rytömaa and P. K. Kinnunen, *J. Biol. Chem.*, 1994, **269**, 1770–1774.